Ind. J. Pharm. Edu. Res., 2026; 60(1):172-182.
https://www.ijper.org

Original Article

Anticancer Effects of Silver Nanoparticles Synthesized from *Eupatorium adenophorum* Extract in Animal Model: Impact on Tumor Growth, Apoptotic Markers and Organ Biomarkers

Shilpa Rana[1], Uddipak Rai[1,*], Vineet Kumar[2], Pankaj Pant[1], Yogita Ale[3]

[1]Department of Pharmacology, Faculty of Pharmacy, DIT University, Dehradun, Uttarakhand, INDIA.
[2]Department of Chemistry and Bioprospecting, Forest Research Institute (FRI), Dehradun, Uttarakhand, INDIA.
[3]Department of Pharmaceutics, Uttaranchal Institute of Pharmaceutical Sciences, Uttaranchal University, Dehradun, Uttarakhand, INDIA.

ABSTRACT

Background: Silver Nanoparticles (AgNPs) synthesized from plant extracts have shown significant anticancer potential. This study explores the efficacy of AgNPs prepared from the methanolic extract of *Eupatorium adenophorum* leaves in treating breast cancer in mice, focusing on their effects on tumor size, weight loss, biochemical markers, and apoptosis-related gene expression. **Materials and Methods:** AgNPs were synthesized and characterized for their size, morphology, and stability. Female BALB/c mice injected with MDA MB231 breast cancer cells were treated with varying doses of AgNPs. Tumor volume and weight loss were measured weekly to assess therapeutic effects and systemic toxicity. **Results:** Weight loss was dose-dependently reduced, with a maximum reduction of 0.4±0.80 g/week at 600 mg/kg EA-AgNP, compared to 0.03±0.01 g/week in the standard group. Tumor inhibition reached 61%, with a 56.25±1.86 mM^3 reduction in tumor volume at the highest dose. Blood glucose levels dropped to 106.25±3.75 mg/dL at 600 mg/kg EA-AgNP, compared to 192.5±2.5 mg/dL in the diseased control group. Apoptotic gene analysis revealed upregulation of pro-apoptotic genes (BAX, caspase-3, and -8) and downregulation of the anti-apoptotic gene (BCL-2), indicating enhanced apoptosis. Biomarker analysis for liver and kidney function showed decreased SGPT, SGOT, uric acid, and urea levels, suggesting a favorable safety profile. Histopathological examination confirmed the absence of malignancy in treated mice. **Conclusion:** AgNPs derived from *Eupatorium adenophorum* exhibit potent anticancer effects in a mouse breast cancer model by promoting apoptosis and reducing tumor growth, underscoring their potential as a promising plant-based therapeutic agent. Further research is needed to elucidate their mechanisms and long-term safety.

Keywords: Cancer, *Eupatorium adenophorum*, MDA MB 231, Murine, Silver nanoparticles, Tumor.

Correspondence:
Dr. Uddipak Rai
Assistant Professor, Department of Pharmacology, Faculty of Pharmacy, DIT University, Dehradun-248009, Uttarakhand, INDIA.
Email: uddipak.rai@gmail.com

Received: 27-11-2024;
Revised: 19-02-2025;
Accepted: 03-06-2025.

INTRODUCTION

Cancer is a hereditary disorder marked by uncontrolled cell growth, division, and spread to other tissues, making it the second leading cause of death globally.[1] Its progression involves evasion of programmed cell death, unchecked replication, angiogenesis, resistance to inhibitory signals, and metastasis.[2] Breast cancer is the most diagnosed cancer in women worldwide and a leading cause of cancer-related deaths, accounting for 27.7% of new cancer cases and 23.45% of deaths among women in India in 2018, as per GLOBOCAN data.[3] Risk factors include advanced age, genetic predisposition, hormonal exposure, lifestyle habits, and environmental pollutants like Polycyclic Aromatic Hydrocarbons (PAHs).[4,5] PAHs, from sources such as vehicular emissions and tobacco smoke, increase breast cancer risk, with 7,12-Dimethylbenz(a)Anthracene (DMBA) commonly used to induce breast cancer in animal models.[6,7] Polycyclic Aromatic Hydrocarbons (PAHs) form due to incomplete combustion of fossil fuels and other carbon-based substances.[8,9] They are emitted from industrial exhaust, vehicle emissions, biomass fuels (e.g., coal burning in rural areas), tobacco smoke, and forest fires. One such PAH, 7,12-Dimethylbenz(a)Anthracene (DMBA), is a carcinogen commonly used to induce breast cancer in rats or mice.[10,11]

DMBA causes oxidative stress, disrupting tissue redox balance, resulting in lipid peroxidation, cellular damage, and pathophysiological changes.[12] Despite advances in anticancer

DOI: 10.5530/ijper.20261036

drugs, challenges like high costs and side effects necessitate safer, cost-effective alternatives. Medicinal plants, rich in bioactive compounds such as terpenoids and flavonoids, show promising therapeutic potential. *Eupatorium adenophorum* (*E. adenophorum*), a plant of the Asteraceae family, exhibits antioxidant, antimicrobial, anticancer, and anti-inflammatory properties, attributed to its phytochemicals like flavonoids and phenolics.[13-15] These compounds show anti-inflammatory, antitumor, and immunomodulatory effects, aiding cancer treatment.[14,16,17] Nanotechnology, particularly Silver Nanoparticles (AgNPs), offers innovative cancer therapies due to their unique physicochemical properties. AgNPs induce Reactive Oxygen Species (ROS), causing oxidative stress, mitochondrial dysfunction, and apoptosis in cancer cells. They also inhibit angiogenesis, impair DNA repair pathways, and enhance immune responses, reducing tumor growth.[18-21] This study evaluates AgNPs synthesized from E. adenophorum methanolic extract for anticancer activity in BALB/c mice injected with MDA MB231 breast cancer cells. Previous research identified methanolic extract as the most effective (via MTT assay) compared to other solvents, with LCMS analysis confirming bioactive compounds. Patented silver nanoparticles (Application No. 202411013021, Publication No. 09/24) were tested for their efficacy in reducing tumor size and improving safety profiles. This highlights the therapeutic potential of E. adenophorum-based AgNPs in breast cancer treatment.

MATERIALS AND METHODS

Animal procurement

At DIT University-faculty of pharmacy, Mussoorie diversion road, Vill-Makkawala, P.O. Bhagwantpur, Dehradun, 248009, Uttarakhand disease-free small animal house, female balb/c mice weighing 25-30 g and aged 3-5 months were bought. The animals were kept in air-conditioned rooms (24°C) with a 12-hr cycle for light and darkness. Female balb/c mice were housed in polypropylene cages that measure 29x15x7 cm, are 2 cm deep in water and have a top wire lid. IAEC (Institutional Animals Ethics Committee) accepted the research protocol. Registration no and date of registration of animal house are 1156/PO/Re/S/07/CPCSEA and 14-june-2021 respectively. Registration no. of our study protocol is 23/06/05.

Collection and Maintenance of Cell Line

The MDA MB 231 cell lines were procured from National Centre for Cell Science, Pune, India. The MDA MB 231 cells were cultured in commonly used media Leibovitz's L-15 medium with 2 mM L-glutamine, supplemented with Fetal Bovine Serum (FBS) and other supplements as required (e.g., glutamine, non-essential amino acids) and aspirated at 37°C and at no carbon dioxide atmosphere.

Chemicals and Reagents

Eosin, Isoflourane, 5- Fluorouracil (5-FU), Dimethyl Sulfoxide (DMSO), Trypan Blue Dye, Haematoxylin Trichloroacetic Acid (TCA), MDA MB 231 Cell Line. All the chemicals were of analytical grade and purchased from Thermo Fischer Scientific and Sigma-Aldrich. The cell line was purchased from NCCS (National Centre for Cell Science) Pune, India.

Formulation Development

The leaves of the plant *Eupatorium adenophorum* were collected in the month of July from Forest Research Institute (FRI), Dehradun, Uttarakhand. The specimen of the plant was submitted to Botanical Survey of India, Dehradun, Uttarakhand for authentication. The accession No. of the specimen is 1302.

Successive extraction of *Eupatorium adenophorum* dried leaves was done via hot percolation method. The methanolic extract was subjected to preparation of silver nanoparticles. For preparation of nanoparticles, 1 M of 20 mL of silver nitrate solution was mixed with 80 mL methanolic leaf extract and was stirred at 40-45°C. After 1.5 hr 0.1 M sodium hydroxide solution was added drop wise till the nanoparticles were prepared. After that solvent was centrifuged, washed and calcinated. Then sample was dried and taken for characterization. The formed nanoparticles were analyzed through SEM, XRD, EDX and FTIR for the confirmation of formation of Silver Nanoparticles (AgNPs).

Tumor Induction

Animals were acclimatized to the environmental condition of lab for at least 1 week before the experiment with adequate supply of food and water and the supply of food and water was stopped 24 hr before the start of the experiment. Total six groups with eight animals in each group were taken for experiment. Except group I all other groups were injected with MDA MB 231 cells ($1*10^6$ cells per mice) by Sub Cutaneous (SC) route in the mammary fat pad of balb/c mice.

Experimental Design

Mice were divided into 6 groups containing eight mice per group (n=8). Group I taken as normal control and treated with DMSO (Dimethyl Sulfoxide) (0.2 mL) only. From group II to VI all mice were injected with MDA MB 231 cells ($1*10^6$ cells per mice) by Subcutaneous (SC) route in the mammary fat pad and this was taken as day zero. Group II served as disease control and was left untreated. Animals in group III was standard group and treated with standard drug 5-Flurouracil (5-FU). After 24 hr of tumor induction group III was given 5-FU at dose of 20 mg/kg dissolved in 10% DMSO via oral route, group IV, V and VI were given dose of *Eupatorium adenophorum* methanol extract Silver Nanoparticles (EA-AgNP) 200 mg/kg, 400 mg/kg and 600 mg/kg respectively as shown in Table 1. The EA-AgNPs were diluted with 10% DMSO then injected on alternative days for five weeks

SC in the mammary fat pad of the mice. From day zero to 5th week life span of all the experimental groups were observed. After the completion of dosing, mice were given mild anesthesia using isoflourane and sacrificed by cervical dislocation at the end of fifth week. Serum was separated for biochemical tests and tissues of breast were fixed in 10% formalin for the histopathological studies and for RTPCR tissues were stored in deep freezer at -80°C.

Evaluation of Weight Loss

In order to assess the extent of weight loss following the introduction of cancer cells, the weight of each mouse was recorded using an electric balance for five consecutive weeks throughout the treatment period. The rate of weight loss was determined by calculating the average value for both control and treated mice using the following equation:[22]

$$\text{The rate of weight loss} = \frac{\text{First day weight} - \text{Last day weight}}{\text{Total day of treatment}} \text{g/day}$$

Cell Growth Inhibition

The assessment of *in vivo* cancer cell growth suppression was performed. Cell growth inhibition is widely used assay to determine the number of cells in a collective sample by using a hemocytometer which can easily separate the live cells from dead cell when using trypan blue dye exclusion.[23] In order to ascertain the prevention of cell growth; 4 groups of mice were subjected to treatment. At the end of the fifth week, each group of mice was euthanized by isoflurane and the cancer cells were extracted and diluted in normal saline (1% NaCl). The enumeration of viable cells was initially conducted using a hemocytometer and trypan blue dye, employing the subsequent equation:[24]

$$cells/_{ml} = \frac{The average count per square \times dilution factor}{depths of fluid under cover slip area acounted}$$

Percentage of cell growth inhibition was calculated by comparing the total number of viable cells in the treated groups with diseased control group using the following equation:[25]

$$\text{Percentage of cell growth inhibition } (\%) = {}^{1 - Tw}/_{Cw} \times 100$$

Where, T_w is mean of number of MDA MB 231 cells of the treated group mice and C_w is mean of number of MDA MB 231 cells of the diseased control group mice.

Measurements of mammary tumor volume

The size of the mammary tumors was assessed using a Vernier caliper scale. The calculation of tumor Volume (V) was performed.

$$V(mm^3) = (L \times B2)/2$$

where L (large diameter) and B (small diameter) are perpendicular, stated in millimeters (mm).[5,26]

Biochemical assay

Effect on glucose level was studied by collecting the blood through cardiac puncture and retro orbital plexus and glucose level was measured using glucometer.[27] The blood was collected from retro orbital plexus on day 0, day 18 and day 35 for estimation of glucose level in blood during the five-week study. The liver function parameters as Serum Glutamic Pyruvate Transaminase (SGPT) and Serum Glutamic Oxaloacetate Transaminase (SGOT) and kidney function parameters, urea and uric acid test were measured according to the method by Reitman and Frankel.[28] The level of Lipid Peroxidation (LPO) was assessed by measuring Thiobarbituric Acid Reactive Substances (TBARS) using the double heating method. This approach is based on the premise of spectrophotometrically measuring the colour created when Thiobarbituric Acid (TBA) reacts with Malondialdehyde (MDA). In this experiment, a centrifuge tube was used to combine 2.5 mL of a 10% solution of Trichloroacetic Acid (TCA) with 0.5 mL of serum. The mixture was then heated in a water bath at a temperature of 90°C for duration of 15 min. After being cooled to room temperature, the mixture was then centrifuged at 3000 rpm for 10 min. Next, 2 mL of the resulting liquid was combined with 1 mL of a 0.675% TBA solution in a test tube. The test tube was then heated in a water bath at 90°C for 15 min, followed by cooling to room temperature. Subsequently, additional absorbance was quantified using a UV-vis spectrophotometer (Thermo Scientific UV-10 USA) at a wavelength of 532 nm.[29]

Histopathological analysis

Small fragments of breast tissue were immersed in a 10% formalin solution for duration of 24 hr. The tissues were subsequently dehydrated using ethanol and then embedded in paraffin. Thin slices of 5 µm in thickness were prepared and treated with

Table 1: Animal groups with their code and the type of treatments.

Groups	Group code	Tumor Induction	Treatment
I	NC (Normal Control).	None	DMSO
II	DC (Diseased Control).	MDA MB 231 cell line.	DMSO
III	ST (Standard).	MDA MB 231 cell line.	5- Fluorouracil (5-FU).
IV	(EA-AgNP2) Treatment group.	MDA MB 231 cell line.	EA-AgNP 200 mg/kg.
V	(EA-AgNP4) Treatment group.	MDA MB 231 cell line.	EA-AgNP 400 mg/kg.
VI	(EA-AgNP6) Treatment group.	MDA MB 231 cell line.	EA-AgNP 600 mg/kg.

haematoxylin and eosin stains. These stained slices were then examined under a light microscope for histological analysis.[30]

Effect on Apoptotic genes (Evaluation through RT-PCR)

The association between apoptosis triggered by EA-AgNP and the expression of certain genes, including Caspase 3, Caspase 8, BAX and BCl2 was identified using RT-PCR. The mRNA was transcribed in reverse to cDNA and cDNA was amplified via real time PCR utilizing sybr green kit. Glyceraldehyde-3-Phosphate Dehydrogenase (GAPDH) was used as a house keeping gene and 35 cycle was run for RTPCR. It catalyzes the Glyceraldehyde-3-Phosphate (G3P) into 1,3-biphosphoglycerate in the presence of inorganic phosphate and NAD^+, which is essentially required in the glycolytic pathway. The sequence of primers used for the amplification of cDNA is shown in Table 2.

Statistical Analysis

The values were expressed as mean±standard error of the mean. Statistical analysis was done using software Prism Graphpad-10 by one-way ANOVA followed by Tukey's multiple comparison test, where ****p<0.0001 considered as very highly significant, ***p<0.001 considered as high significant, **p<0.01 significant, *p<0.05 as least significant and ns as non-significant.

RESULTS

Characterization of Silver Nanoparticles

SEM-EDX Analysis

The shape of the AgNPs was established by the surface topography, which was observed through SEM. The well-defined spherical morphologies of the synthesized AgNPs were observed.

Crystallographic analysis of AgNPs

The size and crystalline phase of biogenic AgNPs are revealed by the XRD results. The Silver nanoparticles diffraction peaks at x axis 39.88, 39.91, 43.65, 78.88 and 65.86 theta confirm that the corresponding intensity is 1515, 1415, 1555, 1000 and 1140 respectively.

FTIR Analysis

The primary functional group implicated in AgNP synthesis was identified via an analysis of the FTIR spectra of biogenic AgNPs. The AgNPs spectra revealed the functional groups involved in stabilizing AgNPs by an absorption peak found at 2879.082, 3011.306, 3742.231 and 3871.890 cm^{-1}.

Evaluation of Weight Loss

The loss in the body weight is one of the symptoms of cancer. The mice used in experiment showed gradual loss in their body weight once they were injected with MDA MB 231 cancer cell lines. The loss in the body weight was found to be 1.775±0.052, 0.033±0.014, 1.037±0.188, 1.137±0.084, 0.4±0.0801 g/week for the DC, ST, EA-AgNP2, EA-AgNP4 and EA-AgNP6 treated groups. Since no cancer was induced in normal control group there was minor weight loss observed with an average weight loss of 0.012±0.002 g/week. The rate of weight loss of EA-AgNP treated mice was seen to be reduced in dose dependent manner with respect to diseased control group, whereas their rate of weight loss was higher than that of standard drug. The data is represented in Figure 1A.

Evaluation of cell growth inhibition

The cells growth inhibitions after the administration of cancer cells in diseased control, standard, EA-AgNP 200 mg/kg, 400 mg/kg and 600 mg/kg each day for consecutive five weeks is represented in Figure 1B. The %age of cell growth inhibition was calculated for DC, ST and treated groups of EA-AgNP2, EA-AgNP4 and EA-AgNP6 and was found to be 11%±0.057, 74%±0.36, 31±0.30%, 58±0.17% and 65±0.13% respectively. Quantification of MDA MB 231 cells using a hemocytometer and trypan blue staining revealed a significant decrease in cell viability in dose dependent manner across all treated groups compared to the diseased control group.

Measurements of mammary tumor volume

Tumor volume was seen with highly significant (****p<0.0001) decrease in ST, significant (**p<0.01) decrease in EA-AgNP6 group whereas least significant (*p<0.05) decrease in EA-AgNP4 and non-significant decrease in EA-AgNP2 treated groups with respect to the DC group. The Figure 1C clearly represents the data. The average tumor volume in DC group was found to be 107.5±4.5 mM^3 whereas in the standard it was found to be 16.5±1.8 mM^3 and in EA-AgNP treated groups tumor volume reduced in a dose dependent manner and calculated as 89.75±1.75 mM^3, 83.5±2.29 mM^3 and 56.25±1.86 mM^3 for 200 mg/kg, 400 mg/kg and 600 mg/kg respectively.

Table 2: Primers sequence used for amplification of cDNA.

Gene	Primer Sequence
BAX	5' TTTGCTTCAGGGTTTCATCCA 3' F 5' CTCCATGTTACTGTCCAGTTCGT 3' R
BCl2	5' CATGTGTGTGGAGAGCGTCAA 3' F 5' CAGATAGGCACCCAGGGTGA 3' R
Caspase 3	5'GTGGAACTGACGATGATATGGC 3'F 5' CGCAAAGTGACTGGATGAACC 3' R
Caspase 8	5' CTGGGAAGGATCGACGACGAT 3' F 5' CATGTCCTGCATTTTGATGG 3' R
GAPDH	5'CGACTTCAACAGCGACACTCAC 3' F 5'CCCTGTTGCTGTAGCCAAATTC 3'R

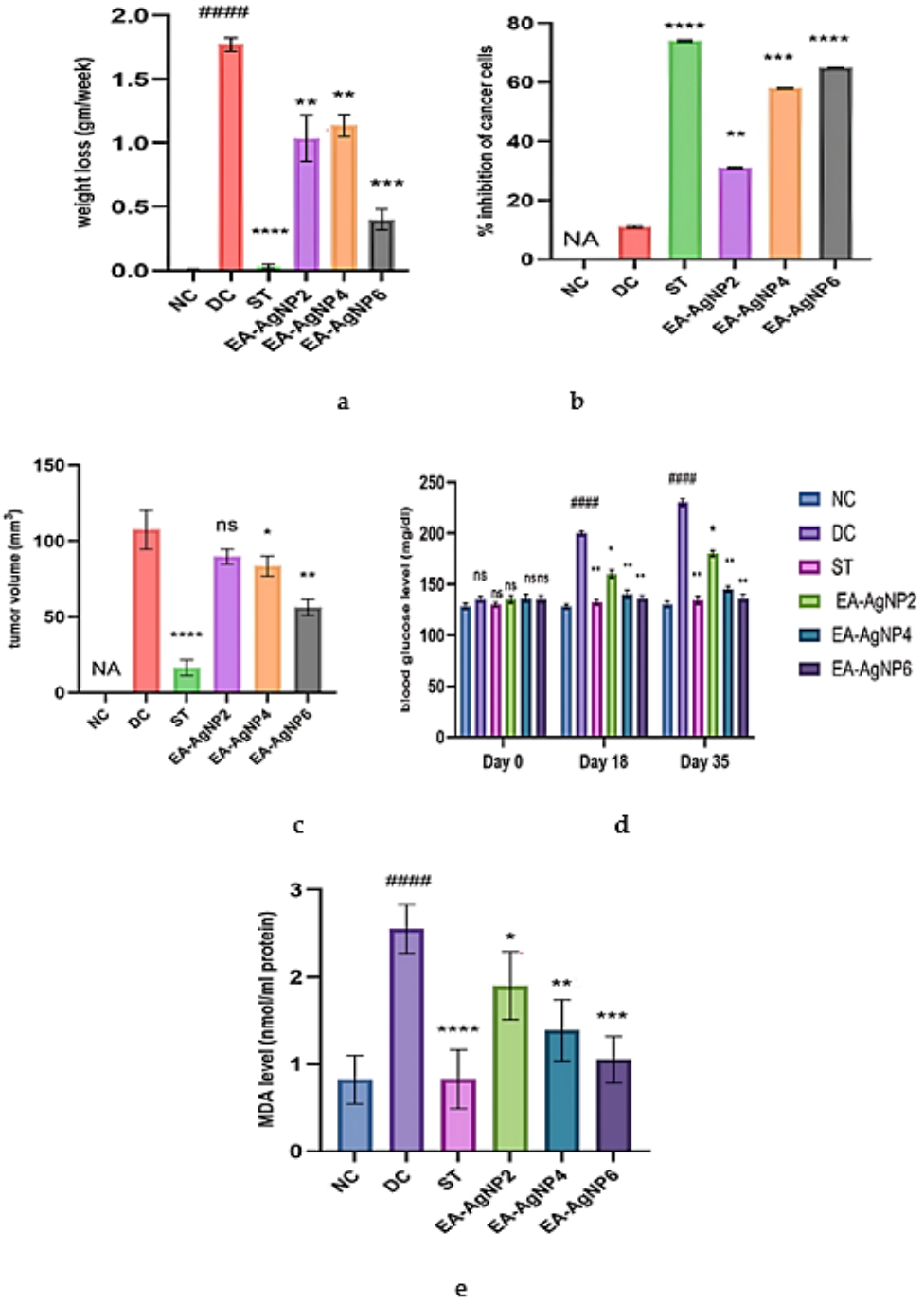

Figure 1: a: Evaluation of weight loss of balb/c mice; All the values are represented as Mean±SEM (n=8), where ****p<0.0001, ***p<0.001 and **p<0.01 represents significant difference, compared to diseased control and ####p<0.0001 represents significant difference, compared to normal control. b: Evaluation of cancer cell inhibition in balb/c mice; All the values are represented as Mean±SEM (n=8), where ****p<0.0001, ***p<0.001 and **p<0.01 represents significant difference, compared to diseased control. c: Evaluation of tumor volume in balb/c mice; All the values are represented as Mean±SEM (n=8), where ****p<0.0001, **p<0.01 and *p<0.05 represents significant difference, compared to diseased control and ns represents non-significant change with respect to disease control. d: Evaluation of blood glucose level of balb/c mice; All the values are represented as Mean±SEM (n=8), where**p<0.01 and *p<0.05represents significant difference, compared to diseased. e: Evaluation of MDA level in balb/c mice; All the values are represented as Mean±SEM (n=8), where (****p<0.0001, ***p<0.001, **p<0.01 and *p<0.05) represents significant difference, compared to diseased control and (####p<0.0001) represent significant difference compared to normal control. NC: Normal Control, DC: Diseased Control, ST: Standard, EA-AgNP2: EA-AgNP 200 mg/kg, EA-AgNP4: EA-AgNP 400 mg/kg, EA-AgNP6: EA-AgNP 600 mg/kg.

Table 3: Effect of different treatments on liver and kidney biomarker parameters.

Parameters	NC	DC	ST	EA-AgNP2	EA-AgNP4	EA-AgNP6
SGPT (u/mL)	37.125±0.51	90.25±1.52***	37.25±1.17###	54.875±0.47ns	50.125±2.64#	39.625±0.98##
SGOT (u/mL)	35.75±0.79	67.625±0.84**	43±0.70##	54.875±0.78ns	47.125±0.51#	44±1.06##
Urea (mg/dL)	27.37±3.09	47.5±1.05**	28±1.40##	39.14±0.99#	38.125±0.95#	36.875±1.37#
Uric acid (mg/dL)	3.74±0.17	6.45±0.24**	3.75±0.25##	4.87±0.30#	5.04±0.33#	4.635±0.30##

All the values are represented as mean ±SEM (n=8), where***p<0.001 and **p<0.01, represents significant difference, compared to normal control and ###p<0.001, ##p<0.01, #p<0.05 and ns(non-significant) represents significant difference, compared to the diseased control group.

SGPT: Serum Glutamic Pyruvic Transaminase, SGOT: Serum Glutamic Oxaloacetic Transaminase.

Measurement of blood glucose level

The average blood glucose level was calculated on day 0, day 18 and day 35 during five weeks of study. On day 0 the blood glucose level was found to be in normal range for all the groups. It was calculated as 128±3.0, 135±3.0 mg/dL, 130±2.15 mg/dL, 135±4.0 mg/dL, 136±4.12 mg/dL and 135±3.10 mg/dL for NC, DC, ST, EA-AgNP2, EA-AgNP4 and EA-AgNP6 groups respectively. On day 18 there was an increase in blood glucose level in DC group with respect to NC group and reduction in blood glucose level was seen in ST and treatment groups with respect to DC group and found to be 128±3.0 mg/dL 200±2.0 mg/dL, 132±3.12 mg/dL, 160±4.0 mg/dL, 140±4.0, 140±3.0 mg/dL and 136±4.0 mg/dL for NC, DC, ST, EA-AgNP2, EA-AgNP4 and EA-AgNP6 groups respectively. On day 35 the blood glucose level was seen as 130±3.0 mg/dL, 230±4.0 mg/dL, 134±4.10 mg/dL, 180±3.0 mg/dL, 145±3.0 mg/dL and 136±4.0 mg/dL for NC, DC, ST, EA-AgNP2, EA-AgNP4 and EA-AgNP6 groups respectively. The significant decrease in blood glucose level was seen in dose dependent manner for treatment groups. The data is represented in Figure 1D.

Effect on liver and kidney biomarker parameters

A significant decrease was observed in liver function i.e. SGPT and SGOT biomarkers and kidney function biomarkers i.e. urea and uric acid level. The SGPT, SGOT, urea and uric acid level of ST group and treatment groups reduced with respect to the DC group in a dose dependent manner. The liver function biomarker and kidney function biomarker parameters showed significant increase in SGPT (***p<0.0001) and SGOT (**p<0.01) level and urea (**p<0.01) and uric acid (**p<0.01) level for DC group when compared to NC group. There was a less significant (##p<0.01), least significant (#p<0.05) and non-significant (ns) decrease in SGPT and SGOT level for EA-AgNP6, EA-AgNP4 and EA-AgNP2 group respectively and significant (p<0.001 and p<0.01) reduction was seen in ST group of SGPT and SGOT respectively when compared to DC. The urea and uric acid level in DC increased less significantly (**p<0.01) when compared to NC. There was significant (##p<0.01, #p<0.5, #p<0.05, #p<0.05) decrease in urea level in ST, EA-AgNP6, EA-AgNP4 and EA-AgNP2 group respectively in comparison to DC. In case of uric acid level significant (##p<0.01, ##p<0.001, #p<0.05, #p<0.05) decrease was seen in ST, EA-AgNP6, EA-AgNP4 and EA-AgNP2 group respectively in comparison to DC. The SGPT, SGOT, urea and uric acid levels for treated groups in comparisons to the diseased control groups are shown in Table 3.

Effect on Lipid per oxidation level

The level of Malondialdehyde (MDA) which is a marker of lipid per oxidation was found to be 0.82±0.09 nmol/mL protein for NC and for DC it was 2.55±0.09 nmol/mL protein which was significantly high (####p<0.0001) with respect to NC. For ST group it was0.825±0.11 nmol/mL protein and the EA-AgNP treated groups showed reduction in a dose dependent manner for MDA and calculated as 1.9±0.13, 1.38±0.12 and 1.05±0.09 nmol/mL protein for EA-AgNP2, EA- AgNP4 and EA-AgNP6 respectively. The data is represented in Figure 1E.

RT PCR Evaluation

The Figure 2 clearly indicate the effect on the expression of genes BAX, BCl2, capase3 and caspase 8 when treated with NC, DC, ST and EA-AgNP treated groups of various concentration. There was a significant decrease in BAX expression in DC group with respect to NC group. An increase in BAX expression was seen in ST group and EA-AgNP treatment group, in dose dependent manner with respect to DC group. BCl2 expression was significantly decreased in all the treated groups and ST group with respect to DC group and BCl2 expression was increased in DC group when compared to NC group. There was a significant increase in caspase 3 and caspase 8 expression in all the EA-AgNP treatment groups and ST group with respect to DC group. All the genetic expressions were obtained and analyzed after normalization with GAPDH housekeeping gene (internal control).

Histopathological study

In the present histopathological examination, Figure 3A the mammary tissue section of NC treated drug, showed ducts and mucin. Section of DC treated mammary tissue showing dedifferentiated cells, ducts and mucin in Figure 3B. In Figure 3C section of ST group showed apoptotic cells. In Figure 3D section of EA-AgNP2 treated group showing apoptotic cells indicating apoptosis of cancer cells and presence of stroma. In Figure 3E

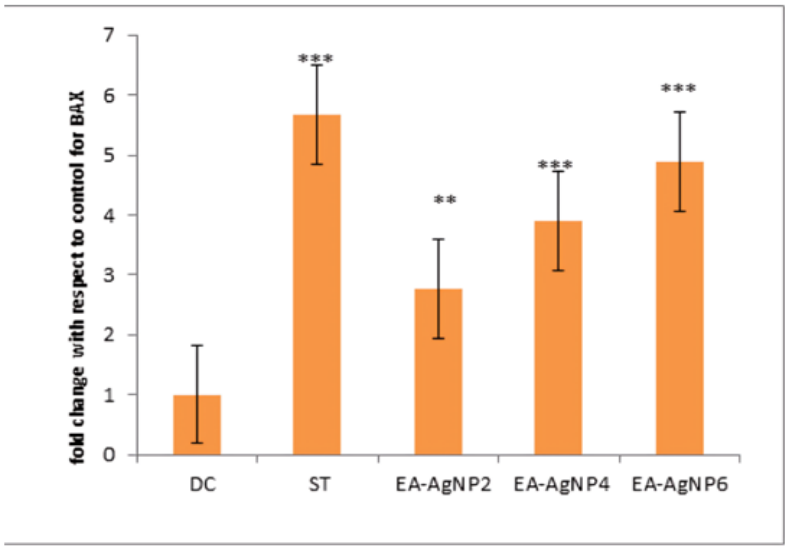
fold change with respect to control for BAX
0
1
2
3
4
5
6
7
***
**
***
***
DC
ST
EA-AgNP2
EA-AgNP4
EA-AgNP6

a

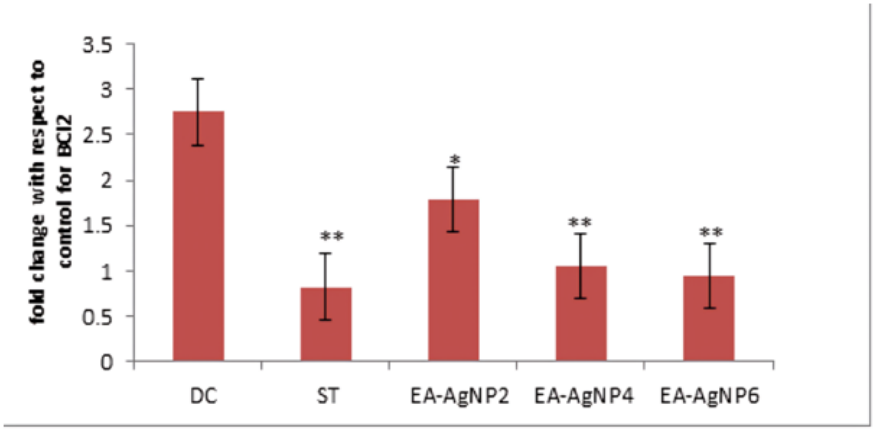
fold change with respect to control for BCl2
0
0.5
1
1.5
2
2.5
3
3.5
**
*
**
**
DC
ST
EA-AgNP2
EA-AgNP4
EA-AgNP6

b

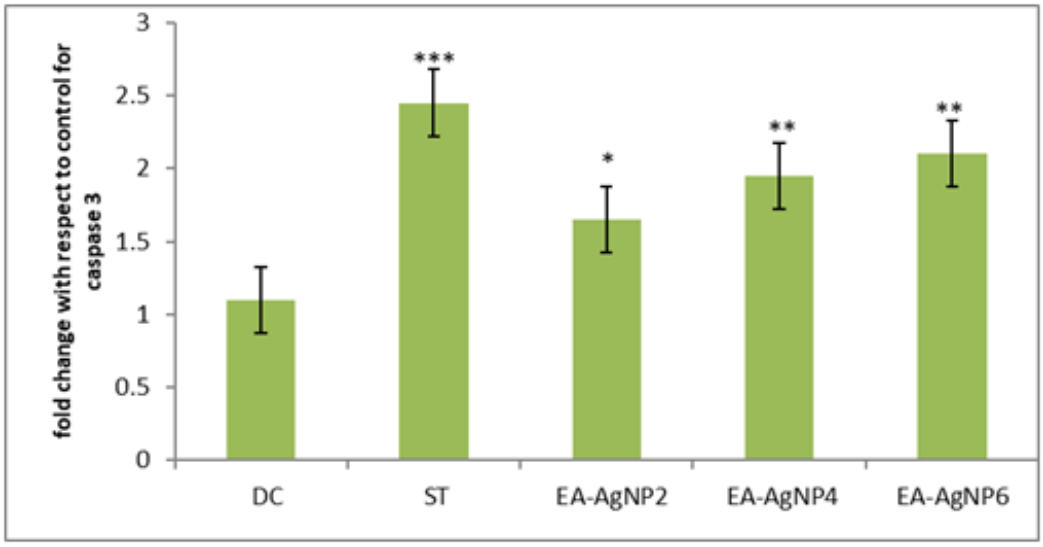
fold change with respect to control for caspase 3
0
0.5
1
1.5
2
2.5
3
***
*
**
**
DC
ST
EA-AgNP2
EA-AgNP4
EA-AgNP6

c

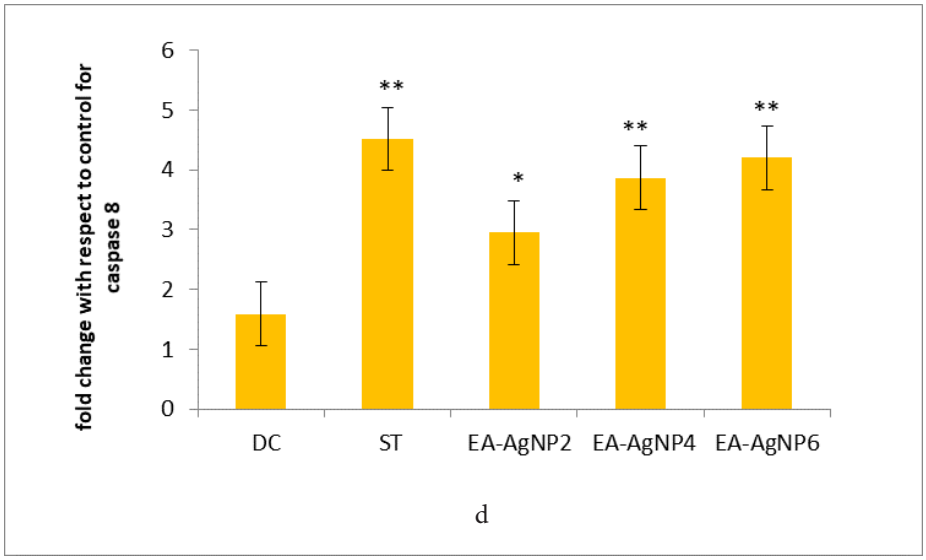

Figure 2: A: Evaluation of BAX gene expression in balb/c mice; All the values are represented as mean±SEM (n=3), where ***p<0.001 and **p<0.1 represents significant difference of standard and treatment groups, compared with diseased control. B: Evaluation of BCl2 gene expression in balb/c mice; All the values are represented as mean±SEM (n=3), where **p<0.01 and *p<0.05 represents significant difference of standard and treatment group, compared with diseased control. C: Evaluation of caspase-3 gene expression in balb/c mice; All the values are represented as mean±SEM (n=3), where ***p<0.001, **p<0.01 and *p<0.05 represents significant difference of standard and treatment group, compared with diseased control. D: Evaluation of caspase-8 gene expression in balb/c mice; All the values are represented as mean±SEM (n=3), where **p<0.01 and *p<0.05 represents significant difference of standard and treatment group, compared with diseased control. DC: Diseased Control, ST: Standard, EA-AgNP2: EA-AgNP 200 mg/kg, EA-AgNP4: EA-AgNP 400 mg/kg, EA-AgNP6: EA-AgNP 600 mg/kg.

section of EA-AgNP4 showed mammary lobules and stroma. In Figure 3F section of EA-AgNP6 treated section showed intact adipose tissue and duct indicating apoptosis of cancer cells.

Microphotograph of mice mammary tissue stained with hematoxylin and eosin. (a) Section of normal control group showing the well differentiated cells in Ducts (D) basement membrane is discontinuous and Mucin (M) is also present and covered with thick mass of fibrous connective tissues, Apoptotic cells (A) are also present. (b) Section of diseased group showing dedifferentiated cells in the Duct (D) and Mucin (M) is over expressed. (c) Section of standard drug treated group showing Apoptotic cells (A), elongated Mucin (M) and well differentiated cells (D). (d) Section of 200 mg/kg EA-AgNP treated mammary tissue, showing Apoptotic cells (A), overexpressed Mucin (M) and dedifferentiated cells in the duct (D). (e) Section of 400 mg/kg EA-AgNP treated mammary tissue showing Apoptotic cells (A), well differentiated cells in ducts (D) and intact Adipose tissue (AD). (f) Section of 600 mg/kg EA-AgNP treated mammary tissue showing intact Adipose Tissue (AD), well differentiated cells in Duct (D) and Apoptotic cells (A).

DISCUSSION

Cancer remains a leading cause of death globally, with current treatments often causing severe side effects. Researchers and pharmaceutical companies are exploring herbal formulations as alternative therapies. *Eupatorium adenophorum* (*E. adenophorum*) has demonstrated anti-cancer properties, and *in vitro* studies have shown the efficacy of its methanolic leaf extract. This research investigates the *in vivo* anticancer potential of Silver Nanoparticles (AgNPs) synthesized from the methanolic extract of *E. adenophorum* leaves. The formulation confirmed AgNP synthesis, with SEM revealing spherical nanoparticles, EDX confirming 68.2% silver content, FTIR identifying functional groups, and XRD indicating crystalline structure Weight loss, a common parameter in cancer studies due to altered metabolism, was significantly (p<0.0001) observed in the Diseased Control (DC) group compared to the Normal Control (NC) group (Figure 1A). Cancer cells can also alter the way body will metabolize the nutrients resulting in inefficient energy use and as a consequence reduction in weight loss.[31] EA-AgNP treatment reduced weight loss dose-dependently, indicating its role as an anticancer agent. Cancer cell inhibition is another critical measure of anticancer activity. Various drugs inhibit cancer by mechanisms such as DNA damage, apoptosis induction, or enzyme inhibition. Some drugs lead to apoptosis by inhibiting anti-apoptotic genes like BCl2 and some drugs are nucleotide analogs that act by inhibiting proper replication and function of DNA as they mimic normal building blocks of DNA or RNA with slightly modified structure.[32] EA-AgNP showed a dose-dependent increase in cancer cell inhibition, with the highest inhibition observed in the Standard Treatment (ST) group using 5-FU (Figure 1B). Tumor volume also significantly decreased in the ST group (p<0.0001), EA-AgNP6 (p<0.01), EA-AgNP4 (p<0.05), and nonsignificantly in EA-AgNP2-treated groups compared to DC (Figure 1C). Cancer cells often exhibit elevated blood glucose levels due to their high metabolic rate. Cancer cells have a high metabolic rate and often rely on glycolysis for energy production. This increased

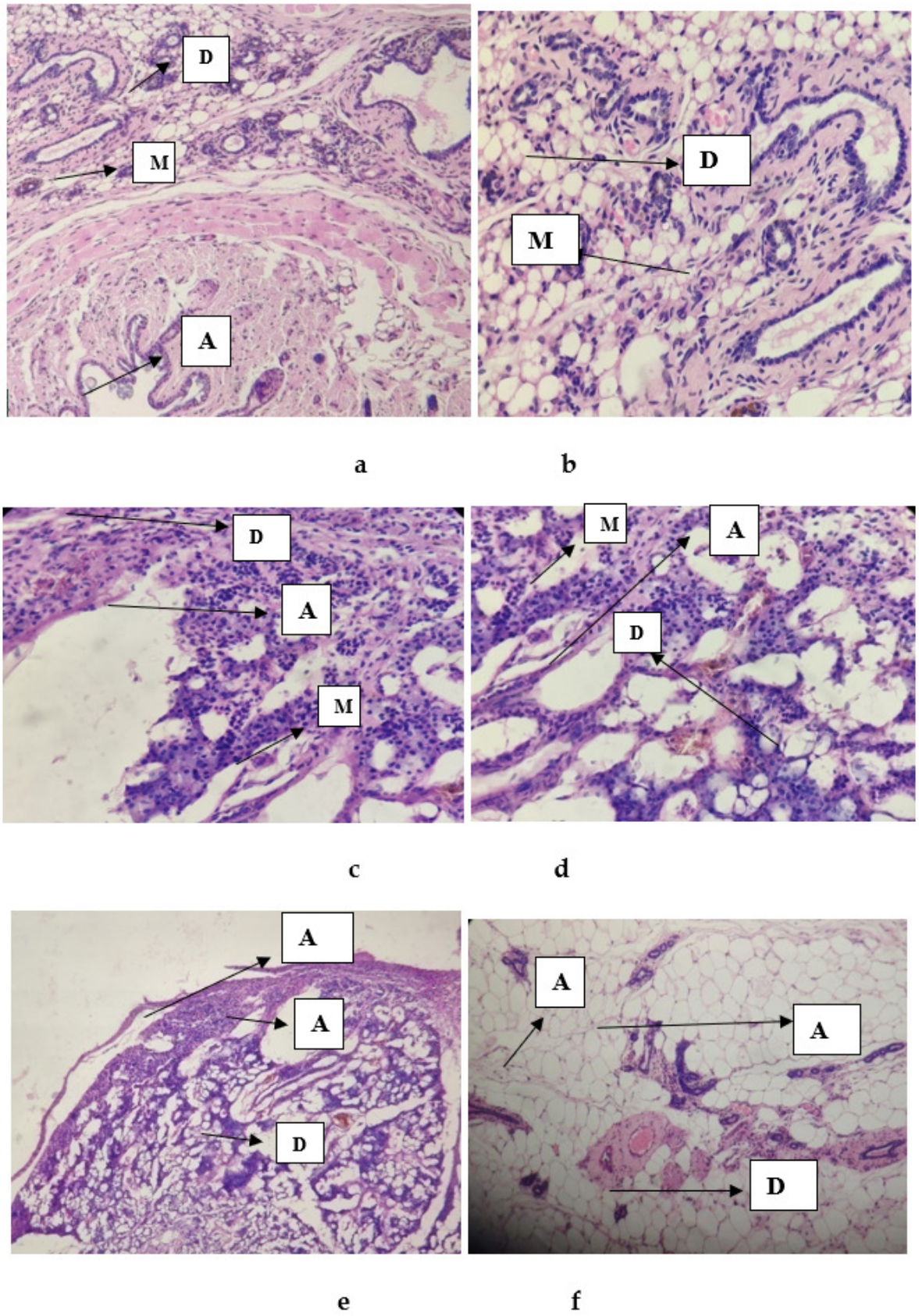

Figure 3: The section of mammary tissue seen in 100X magnification. A: NC (DMSO treated). B: DC (MDA MB231 treated). C: ST (MDA MB231+5-FU treated). D: EA-AgNP (MDA MB231+200 mg/kg EA-AgNP). E: EA-AgNP4(MDA MB231+400 mg/kg EA-AgNP). F: EA-AgNP6 (MDA MB231+600 mg/kg EAAgNP).

demand for glucose leads to elevated blood glucose level as the body attempts to supply the growing tumor with sufficient energy.[33] No significant change in glucose levels was observed on day 0, but levels increased significantly ($p<0.0001$) in the DC group on days 18 and 35. EA-AgNP treatments reduced glucose levels dose-dependently, with significant reductions ($p<0.01$ for EA-AgNP6 and EA-AgNP4, $p<0.05$ for EA-AgNP2) compared to DC. Liver and kidney biomarkers (SGOT, SGPT, urea, and uric acid) were evaluated (Table 3). EA-AgNP treatments significantly reduced these biomarkers, with the highest concentration (600 mg/kg) showing the most pronounced effects. Lipid peroxidation, a marker of oxidative stress, was assessed using Malondialdehyde (MDA). Oxidative stress is frequently increased in cancer as a result of the elevated metabolic rate of rapidly dividing cells and the presence of inflammation in the tumor microenvironment.[34] Cancer-induced oxidative stress increased MDA levels significantly ($p<0.0001$) in DC. EA-AgNP treatments reduced MDA levels dose-dependently (Figure 1E), highlighting their antioxidant and anticancer efficacy. Apoptosis-related genes (BAX, BCl2, caspase-3, and caspase-8) were also examined. Caspase-8 initiates the apoptotic signal in response to extrinsic factors and caspase-3 executes cell death program by degrading key cellular components.[35] BAX, caspase-3, and caspase-8 expression increased significantly in EA-AgNP-treated groups, while BCl2 expression decreased compared to DC. EA-AgNP6 showed the most significant changes in these genes, promoting apoptosis in cancer cells (Figures 2a-2d). Histological analysis of breast cancer tissues (Figure 3) revealed dedifferentiated cells in DC, apoptotic cells in ST and EA-AgNP2 groups, and defined mammary lobules with intact adipose tissue in the EA-AgNP6 group, confirming its efficacy in reducing cancer progression at higher concentrations.

CONCLUSION

Therefore, considering all the data, it can be inferred that the silver nanoparticles of methanolic extract obtained from *Eupatorium adenophorum* leaves has anti-proliferative action, effectively inhibiting the growth rate of breast tumors in the mice model. The plant extract also has a beneficial impact on the liver and kidneys. Consequently, it can be identified as potential and safe anticancer medication specifically targeting breast cancer.

ACKNOWLEDGEMENT

The authors would like to thank the Chancellor, Vice Chancellor and Director of Faculty of Pharmacy, School of Pharmaceutical and Population Health Informatics, DIT University, Dehradun, India for providing the labs for the successful conduction of this research work.

CONFLICT OF INTEREST

The authors declare that there is no conflict of interest.

ABBREVIATIONS

AgNPs: Silver nanoparticles; ***E. adenophorum*:** *Eupatorium adenophorum*; **EA-AgNP:** *Eupatorium adenophorum* silver nanoparticles; **BAX:** Bcl-2-associated X protein; **Bcl-2:** B cell lymphoma-2; **PAHs:** Polycyclic Aromatic Hydrocarbons; **DMBA:** 7;12-Dimethylbenz(a)Anthracene; **ROS:** Reactive Oxygen Species; **SGPT:** Serum Glutamic Pyruvate Transaminase; **SGOT:** Serum Glutamic Oxaloacetate Transaminase; **LPO:** Lipid Peroxidation; **TBARS:** Thiobarbituric Acid Reactive Substances; **TBA:** Thiobarbituric Acid; **MDA:** Malondialdehyde; **TCA:** Trichloroacetic Acid; **NC:** Normal Control; **DC:** Diseased Control; **ST:** Standard; **EA-AgNP2:** *Eupatorium adenophorum* Silver nanoparticles 200 mg/kg; **EA-AgNP4:** *Eupatorium adenophorum* Silver nanoparticles 400 mg/kg; **EA-AgNP6:** *Eupatorium adenophorum* Silver nanoparticles 600 mg/kg; **MTT:** 3-[4,5-dimethylthiazol-2-yl]-2,5 diphenyl tetrazolium bromide; **IC_{50}:** Inhibitory concentration 50; **DMSO:** Dimethyl sulfoxide; **RTPCR:** Real-time Polymerase Chain Reaction; **GAPDH**: Glyceraldehyde-3-phosphate Dehydrogenase.

SUMMARY

The silver nanoparticles were developed from the methanolic extract of *Eupatorium adenophorum* leaves. These nanoparticles of different concentrations were induced into the female balb/c mice and various parameters for cancer were studied. The drug showed improvement in the inhibition of cancer in a dose dependent manner for the formulation. Significant decrease in weight, blood glucose, MDA, cancer cell growth, SGOT, SGPT, Urea and uric acid level was seen by EA-AgNP6. BAX, Caspase-3, -8 significantly increased, BCL2 significantly decreased by EA-AgNP6. Histopathology showed presence of intact adipose tissue by EA-AgNP6, indicating decrease in cancer cells.

ETHICAL STATEMENT

Approval from Institutional Animal Ethics Committee (IAEC) was taken. Registration No. of our study protocol is 23/06/05.

REFERENCES

1. Bray F, Ferlay J, Soerjomataram I, Siegel RL, Torre LA, Jemal A. Global cancer statistics 2018: GLOBOCAN estimates of incidence and mortality worldwide for 36 cancers in 185 countries. CA Cancer J Clin. 2018; 68(6): 394-424.
2. Hanahan D, Weinberg RA. The hallmarks of cancer. Cell. 2000; 100(1): 57-70.
3. Łukasiewicz S, Czeczelewski M, Forma A, Baj J, Sitarz R, Stanisławek A. Breast cancer-epidemiology, risk factors, classification, prognostic markers and current treatment strategies-an updated review. Cancers (Basel). 2021; 13(17): 4287.
4. Ferlay J, Ervik M, Lam F, Colombet M, Mery L, Pineros M, *et al.* Estimating the global cancer incidence and mortality in 2018: GLOBOCAN sources and methods. Int J Cancer. 2019; 144(8): 1941-53.
5. Akhouri V. Therapeutic effect of *Aegle marmelos* fruit extract against DMBA induced breast cancer in rats. Int J Sci Res Sci Technol. 2018; 4(2): 1050-6.
6. Kim JH, Lee J, Jung SY, Kim J. Dietary factors and female breast cancer risk: A prospective cohort study. Nutrients. 2017; 9(12): 1331.
7. Lee DG, Kang D, Lee HJ, Park SK, Lee JE, Oh SM, *et al.* Women's occupational exposure to polycyclic aromatic hydrocarbons and risk of breast cancer. Occup Environ Med. 2019; 76(1): 22-9.
8. Brisken C, Hess K, Jeitziner R. Progesterone and overlooked endocrine pathways in breast cancer pathogenesis. Endocrinology. 2015; 156(10): 3442-50.
9. Rengarajan T, Rajendran P, Nandakumar N, Lokeshkumar B, Rajendran P, Nishigaki I. Exposure to polycyclic aromatic hydrocarbons with special focus on cancer. Asian Pac J Trop Biomed. 2015; 5(3): 182-9.
10. Barros AC, Muranaka EN, Mori LJ, Pelizon CH, Iriya K, Gioconda B. Induction of experimental mammary carcinogenesis in rats with 7,12-dimethylbenz(a) anthracene. Rev Hosp Clin Fac Med Sao Paulo. 2004; 59(5): 257-61.

11. Tatar O, Ilhan N, Ilhan N, Susam S, Ozercan IH. Is there any potential anticancer effect of raloxifene and fluoxetine on DMBA-induced rat breast cancer?. J Biochem Mol Toxicol. 2019; 33(6).
12. Lin Y, Han W, Kim J, You H, Kim MK, Shih WJ, *et al.* Role of mammary epithelial and stromal P450 enzymes in the clearance and metabolic activation of 7,12-dimethylbenz(a)anthracene in mice. Toxicol Lett. 2012; 212(2): 97-105.
13. Krishnamoorthy D, Sankaran M. Modulatory effect of Pleurotus ostreatus on oxidant/antioxidant status in 7,12-dimethylbenz(a)anthracene induced mammary carcinoma in experimental rats-a dose-response study. J Cancer Res Ther. 2016; 12(1): 386-92.
14. Giri S. An updated review on *Eupatorium adenophorum Spreng*. [*Ageratina adenophora* (Spreng.)]: traditional uses, phytochemistry, pharmacological activities and toxicity. J Ethnopharmacol. 2018; 224: 106-22.
15. Liu PY, Liu D, Li WH, Zhao T, Sauriol F, Gu YC, *et al.* Chemical constituents of plants from the genus *Eupatorium* (1904-2014). Chem Biodivers. 2015; 12(10): 1481-515.
16. Islam MS. *In vivo* anticancer activity of *Basella alba* leaf and seed extracts against Ehrlich's ascites carcinoma (EAC) cell line. J Pharm Sci Innov. 2019; 8(4): 141-6.
17. Kabir SR, Nabi MM, Haque A, Zaman RU, Mahmud ZH, Reza MA. Pea lectin inhibits growth of Ehrlich ascites carcinoma cells by inducing apoptosis and G2/M cell cycle arrest *in vivo* in mice. Phytomedicine. 2013; 20(14): 1288-96.
18. Sharifi-Rad M, Pohl P, Epifano F. Phytofabrication of silver nanoparticles (AgNPs) with pharmaceutical capabilities using *Otostegia persica* (Burm.) Boiss. leaf extract. Nanomaterials. 2021; 11(4): 1045.
19. Singh A, Kaur K. Biological and physical applications of silver nanoparticles with emerging trends of green synthesis; engineered nanomaterials-health and safety. J King Saud Univ Sci. 2020; 32(3): 103-8.
20. Abass Sofi M, Sunitha S, Ashaq Sofi M, Khadheer Pasha SK, Choi D. An overview of antimicrobial and anticancer potential of silver nanoparticles. J King Saud Univ Sci. 2022; 34(3): 101791.
21. Sharma NK. Green route synthesis and characterization techniques of silver nanoparticles and their biological adeptness. J Chem Educ. 2019; 96(4): 686-93.
22. Aruoma OI. Free radicals, oxidative stress and antioxidants in human health and disease. J Am Oil Chem Soc. 1998; 75(2): 199-212.
23. Elston CW, Ellis IO. Pathological prognostic factors in breast cancer. I. The value of histological grade in breast cancer: experience from a large study with long-term follow-up. Histopathology. 2002; 41(3): 151-2.
24. Sumitra C, Nagani K. *In vitro* and *in vivo* methods for anticancer activity evaluation and some Indian medicinal plants possessing anticancer properties: an overview. J Pharmacogn Phytochem. 2013; 2(2): 140-52.
25. Mukherjee PK, Kumar V, Houghton PJ. Screening of Indian medicinal plants for acetylcholinesterase inhibitory activity. Phytother Res. 2007; 21(12): 1142-5.
26. Agetia GC, Venkatesh P, Baliga MS. *Aegle marmelos* (L.) Correa inhibits the proliferation of transplanted Ehrlich ascites carcinoma in mice. Biol Pharm Bull. 2005; 28(1): 58-64.
27. Trinder P. Determination of blood glucose using an oxidase-peroxidase system with a non-carcinogenic chromogen. J Clin Pathol. 1969; 22(2): 158-61.
28. Reitman S, Frankel S. A colorimetric method for the determination of serum glutamic oxalacetic and glutamic pyruvic transaminases. Am J Clin Pathol. 1957; 28(1): 56-63.
29. Draper HH, Hadley M. Malondialdehyde determination as index of lipid peroxidation. Methods Enzymol. 1990; 186: 421-31.
30. Miyashita T, Krajewski S, Krajewska M, Wang HG, Lin HK, Liebermann DA, *et al.* Tumor suppressor p53 is a regulator of bcl-2 and bax gene expression *in vitro* and *in vivo*. Oncogene. 1994; 9(6): 1799-805.
31. Hynes O, Anandavadivelan P, Gossage J, Johar AM, Lagergren J, Lagergren P. The impact of pre- and post-operative weight loss and body mass index on prognosis in patients with oesophageal cancer. Eur J Surg Oncol. 2017; 43(8): 1559-65.
32. DeVita VT, Lawrence TS. DeVita, Hellman and Rosenberg's cancer: Principles and practice of oncology. 11th ed. Philadelphia: Wolters Kluwer; 2018.
33. Ediriweera MK, Jayasena S. The role of reprogrammed glucose metabolism in cancer. Metabolites. 2023; 13(3): 345.
34. Aboelella NS, Brandle C, Kim T, Ding ZC, Zhou G. Oxidative stress in the tumor microenvironment and its relevance to cancer immunotherapy. Cancers. 2021; 13(5): 986.
35. Wolf P, Schoeniger A, Edlich F. Pro-apoptotic complexes of BAX and BAK on the outer mitochondrial membrane. Biochim Biophys Acta Mol Cell Res. 2022; 1869(10): 119317.

Cite this article: Rana S, Rai U, Kumar V, Pant P, Ale Y. Anticancer Effects of Silver Nanoparticles Synthesized from *Eupatorium adenophorum* Extract in Animal Model: Impact on Tumor Growth, Apoptotic Markers and Organ Biomarkers. Indian J of Pharmaceutical Education and Research. 2026;60(1):172-82.